Self-Scheduling Robust Preview Controllers for Path Tracking and Autonomous Vehicles

Conference Paper · December 2017

DOI: 10.1109/ASCC.2017.8287452

CITATIONS
2

READS
227

5 authors, including:

Ali Boyali
33 PUBLICATIONS **159** CITATIONS
SEE PROFILE

Vijay John
Toyota Technological Institute
50 PUBLICATIONS **380** CITATIONS
SEE PROFILE

Lyu Zheming
Toyota Technological Institute
4 PUBLICATIONS **10** CITATIONS
SEE PROFILE

Swarn singh Rathour
Toyota Technological Institute
12 PUBLICATIONS **14** CITATIONS
SEE PROFILE

Self-Scheduling Robust Preview Controllers for Path Tracking and Autonomous Vehicles

Ali Boyali, Vijay John, Zheming Lyu, Rathour Swarn and Seichi Mita
Research Center for Smart Vehicles, Toyota Technological Institute, Nagoya, Aichi-Japan
Email:{aliboyali, vijayjohn, lyuzheming, swarn, smita}@toyota-ti.ac.jp

***Abstract*—In this study, we detail the procedures for designing preview gain scheduling controllers by Linear Quadratic H_∞ robust optimization methods in Linear Matrix Inequalities (LMI) framework. The controllers are aimed for steering control of autonomous vehicle. We first construct the Linear Parameter Varying (LPV) vehicle models and synthesize the robust controllers with uncertainty and nominal plants. We choose static output and state feedback controller structure to avoid higher order controllers considering implementation issues. The robust control problems are solved by using different LMI formulations and optimization weights with and without eigenvalue location constraints. The results are compared.**

I. Introduction

The vehicle steering control for path tracking has been broadly studied. In the literature there are wide variety of vehicle dynamics lateral controllers proposed for steering which meet many performance criteria. However, the maximum performance we can get from the controllers are limited with the parameter uncertainty in the vehicle models, varying operating conditions and available information to the controller.

In this paper, we propose robust self-scheduling preview controllers for path tracking. The preview control differs from the Model Predictive Control (MPC) in many aspects. In the preliminary reviews, the reviewers confused the predictive and preview controllers. In the MPC methods, the system model is used to propagate the state space equations through out a prediction horizon predicting the future evolution of the states, and the resulting matrix system is used to solve optimizing input sequence for a given control horizon. The resulting optimization problem is either solved in real time or the offline solution is stored in tables. The latter is called as explicit MPC and the control is taken from look-up tables in operation. However, in the preview control methods, there is no need neither to solve a real time optimization problem nor storing the solutions in look up tables. It is shown that, the preview control and MPC gives identical results [1] for modeling driver steering control applications. There is neither real time prediction nor optimization in the preview control. Therefore, the preview controllers are more easily realizable then the MPC controllers for real time steering control applications.

The history of preview control dates back to 1960's and a plethora of literature on the topic is available. The preview control method we adapted is based on the optimal regulation and servo tracking problem with known input sequence which are theoretically discussed in the optimal control books [2, 3]. First applications of the preview control to the path tracking automated driving problems were reported in [4, 5] for four wheel and front wheel steering passenger cars. These studies were designed for only constant vehicle speeds. The uncertainty on the models as well as the parameter variations were not taken into account.

This paper extends the preview steering controllers by including both parameter variation and uncertainty in the controller design. We contribute to the literature in preview steering control and automated driving with the following solutions;

- All the previous steering controllers were proposed for single vehicle speed operating point. We introduce Linear Parameter Varying (LPV) modeling approach and gain scheduling preview steering control by this paper.
- There is no robust control synthesis for preview steering path tracking problems. In this paper we formulate the problem as a robust control problem and solve in Linear Matrix Inequalities (LMI) framework.
- There is only one LPV-LMI preview control application applied to servomechanism design [6] in which the fast transient dynamics and pole constraints of the controller are not formulated. In this study, we also extend their approach by adding pole constraints to the LMI formulation which results smooth transient modes. The system and preview controller parts are shaped via Lyapunov matrix partitions.

The rest of the paper is organized as following. In Section II, we give brief background information about preview control and its application to vehicle steering and path tracking problem. The LQ H_∞ synthesis and robust control of LPV vehicle system are detailed in Section III. In Section IV, the simulation results and comparison are discussed. The paper ends with the conclusion.

II. Optimal Preview Control

A. Linear Quadratic (LQ) Preview Control

The reference tracking problem in control theory deals with how to make a system to follow a desired trajectory. If the

reference is an output of another system which is known in advance, the problem can be cast into preview control problem and solved by optimization methods. The solution to preview control is formulated as a LQ optimization problem in [3]. The finite and infinite time (time invariant) solutions are obtained by choosing an appropriate cost function and weights (Q for states and R control effort) relating the two systems by state augmentation.

The preview LQ solution was first employed for a vehicle suspension system control and described in [7–9] then the applications extended to the motorcycle and car steering control problems [5, 10]. In this paper we closely follow [10] for vehicle-road model development.

In [10], the road is taken as the path generating plant (1). The vehicle (2) follow the output of this plant.

$$x_r(k+1) = A_r x_r(k) + B_r y_{ri}(k) \qquad y_r(k) = C_r x_r(k) \tag{1}$$

$$x_v(k+1) = A_v x_v(k) + B_v u_v(k) \qquad y_v(k) = C_v x_v(k) + D_v u_v(k) \tag{2}$$

In Equation (1), A_r, B_r and C_r are given by Equation (3) and y_{ri} is the single reference input enters to the system at the preview horizon. The variable y_{ri} is the road state and it represents the deviation of the path preview point at the horizon in the vehicle coordinate system.

$$A_g = \begin{bmatrix} 0 & 1 & 0 & \dots & 0 \\ 0 & 0 & 1 & \dots & 0 \\ \vdots & \vdots & & \ddots & \\ 0 & 0 & 0 & 0 & 1 \\ 0 & 0 & 0 & 0 & 0 \end{bmatrix}_{NxN} \quad B_g = \begin{bmatrix} 0 \\ 0 \\ \vdots \\ 0 \\ 1 \end{bmatrix}_{Nx1} \quad C_g = \begin{bmatrix} 1 \\ 0 \\ 0 \\ \vdots \\ 0 \end{bmatrix}^T \tag{3}$$

The vehicle model equations (2) are derived from the single track vehicle model for the lateral motion (Fig. 1). The vehicle local (x_v, y_v) and the global coordinate frames (X_w, Y_w) are shown in the figure. The vehicle local longitudinal and lateral speed are represented by the variables V_x and V_y respectively.

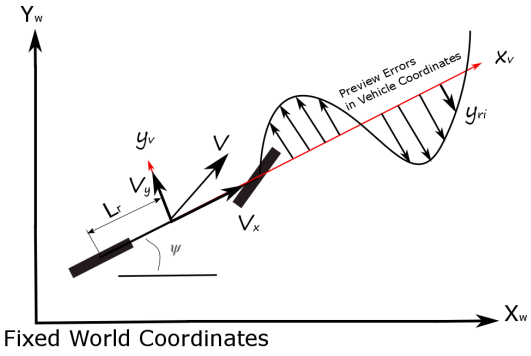

Fig. 1. Single Track Model and Road Preview

The path tracking error is computed with respect to the vehicle local or global coordinates systems, therefore the appropriate single track model defined in the global and local coordinates should be used for the augmented system. We will give only the error model in local coordinate system for brevity in this paper.

The vehicle error model is given as described in [11];

$$\Sigma_t = \begin{cases} x_{ve}(k+1) = A_{ve}x_{ve}(k) + B_v u_v(k) + B_{\dot\psi}\dot\psi_{des}(k) \\ y_{ve}(k) = C_{ve}x_{ve}(k) + D_{ve}u_v(k) \end{cases} \tag{4}$$

where the error state transition A_{ve}, disturbance and steering input matrices B_v and $B_{\dot\psi}$ are;

$$A_{ve} = \begin{bmatrix} 0 & 1 & 0 & 0 \\ 0 & -\frac{2(C_{\alpha f}+C_{\alpha r})}{mV_x} & a_{23} & \frac{2(C_{\alpha f}L_f - C_{\alpha r}L_r)}{mV_x} \\ 0 & 0 & 0 & 1 \\ 0 & -\frac{2(C_{\alpha f}L_f - C_{\alpha r}L_r)}{I_z V_x} & a_{43} & -\frac{2(C_{\alpha f}L_f^2 + C_{\alpha r}L_r^2)}{I_z V_x} \end{bmatrix} \tag{5}$$

$$B_{\dot\psi} = \begin{bmatrix} 0 \\ -V_x - \frac{2(C_{\alpha f}L_f - C_{\alpha r}L_r)}{mV_x} \\ 0 \\ -\frac{2(C_{\alpha f}L_f^2 + C_{\alpha r}L_r^2)}{I_z V_x} \end{bmatrix} \quad and \quad B_v = \begin{bmatrix} 0 \\ \frac{2C_{\alpha f}}{m} \\ 0 \\ \frac{2C_{\alpha f}L_f}{I_z} \end{bmatrix} \tag{6}$$

Here,

$$D_{ve} = [0]_{4x2} \quad a_{23} = \frac{2(C_{\alpha f}+C_{\alpha r})}{m} \quad a_{23} = \frac{2(C_{\alpha f}L_f - C_{\alpha r}L_r)}{I_z}$$

In the equations, $C_{\alpha(f,r)}$ are the front and rear cornering stiffness of the tires, $L_{f,r}$ are the distance of the center of gravity of the car to the front and rear axles and $[m, I_z]$ are the mass and moment of inertia of the vehicle around vehicle's z axis respectively. The error states from the desired motion $x_v = \begin{bmatrix} y, & V_y, & \Psi, & \dot\Psi \end{bmatrix}^T$ are the lateral displacement and velocity, heading (yaw) angle and rate in vehicle coordinate system. The road states (x_r) contain only the lateral deviation values in the local coordinate frame. The two systems can now be state augmented in (7) to develop an optimal control law by the classical LQR solutions.

$$\begin{bmatrix} x_{ve}(k+1) \\ x_r(k+1) \end{bmatrix} = \begin{bmatrix} A_{ve} & 0 \\ 0 & A_r \end{bmatrix} \begin{bmatrix} x_{ve}(k) \\ x_r(k) \end{bmatrix} + \begin{bmatrix} B_v \\ 0 \end{bmatrix} u_v(k) + \begin{bmatrix} 0 \\ B_r \end{bmatrix} y_{ri} \tag{7}$$

In the state space equations (7), there is no connection between the road and vehicle states. The augmented discrete states are connected with the new measurement matrix C_{aug} to obtain the cost function to be optimized.

$$\begin{bmatrix} x_{aug}(k+1) \\ y_{aug}(k+1) \end{bmatrix} = \begin{bmatrix} A_{aug}x_{aug}(k) + B_{r.aug}y_{ri} + B_{v.aug}u_v(k) \\ C_{aug}x_{aug}(k) + D_{v.aug}u_v(k) \end{bmatrix} \tag{8}$$

where $x_{aug}(k) = \begin{bmatrix} x_{ve}(k) & y_r(k) \end{bmatrix}^T$.

The road plant provides next preview point and current vehicle heading information to the vehicle at the current time step. Thus the deviation from the next target point $\Delta y = y(k) - y_{r1}$ and current heading angle $\Psi \cong \frac{\Delta y}{V_x T}$ are used for the measurement matrix in the augmented error model. In the equation T is the sampling period. In this case the measurement matrix C_{aug} is expressed as;

$$C_{aug} = \begin{bmatrix} 1 & 0 & 0 & 0 & -1 & 0 & 0 & \dots & 0 \\ 0 & 0 & 1 & 0 & \frac{1}{V_x T} & -\frac{1}{V_x T} & 0 & \dots & 0 \end{bmatrix}$$

The discrete time cost function (Equation 9) is constructed based on the measurement matrix with the appropriate weights on the outputs.

$$J(x(t_0), u(.), t_f)) = \sum_{k=0}^{k=N} [(x_{aug})^T C_{aug}^T Q C_{aug}(x_{aug}) + u_v^T R u_v] dt \tag{9}$$

Here (9) Q is a positive semi-definite matrix containing weights on the diagonal for each measured states while the scaler R is a positive scalar for the control effort. If the assumptions that $[A_{aug}, B_v]$ are stabilisable and $[A_{aug}, C_{aug}]$ detectable hold, the optimal input is computed as $u^*(k) = -Kx_{aug}$. In this case, the state feedback and feedforward controller coefficients are obtained from;

$$K = [K_v, K_r] = (R + B_{v.aug}^T P B_{v.aug})^{-1} B_{v.aug}^T P A_{aug} \quad (10)$$

The gains $[K_v, K_r]$ are the state feedback and feedforward control coefficients for the vehicle and road states respectively and the matrix P satisfies the Discrete Algebraic Riccati Equation (DARE). The analytic computation of the finite time solutions can be found in the references [8, 9] in detail.

The preview horizon at which the feed-forward coefficients go zero, depends on the optimization state Q and control weighting R matrices. These weights are adjusted according to the desired response. Although the preview LQ control methods provide many advantage in tracking control, they cannot be applied verbatim for LPV systems. In the following sections, after a brief review of the robust control of LPV plants, we elaborate the LQ H_∞ synthesis with gain scheduling.

B. Robust Preview Controllers, Previous Studies

The advantage of the preview controllers sparkled many study for application of the method in generalized settings for mixed stochastic LQ/H_2 and LQ/H_∞ controllers [12–14]. Almost all of the proposed controllers are based on the partitioning Riccati solution then obtaining the H_2 and H_∞ controllers from the Hamiltonian matrix analytically [14–16]. A few studies propose classical gain scheduling with preview control in which the controller coefficients are computed at the frozen operating grid points. In [17], the authors use the tire parameters as the scheduling parameter.

A frequency shaped LQ Preview controller is given in [18] with the same scheduling variable. The controller coefficients for both preview and the tracking plants are computed in LMI framework. In this study, there is no pole constraint to prevent fast transient dynamics. There are other studies that use the LMI framework in preview control applications, however in these studies, only the feed-forward part of the controllers are computed by LMI methods [19].

In this paper, we formulated the robust steering controller in a similar manner given in [6] for servo-mechanism controller design. In addition to formulating the controllers and solving the problem in LMI framework, we included pole placement constraints to assign the poles of the closed loop system matrix in the desired LMI region. The longitudinal speed of the vehicle is taken as the scheduling variable.

III. Speed Scheduled Robust Controllers

In the last decades, the LMI based controller design became a community standard as it allows formulating diverse control problems in a flexible manner. In this paper we formulated the preview control problem in classical robust control theory and solved the resulting matrix inequalities with a highly efficient solver (MOESP [20]) in YALMIP framework [21]

In robust controller design, the main objective is to reduce the magnitude of the system norms for the specific input-output channels. The general configuration of the system is given in Fig. (2).

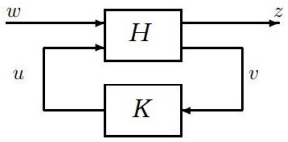

Fig. 2. Robust Control Generalized Plant

The figure shows a generalized plant (H) with a controller (K) which are connected via a feedback loop. The signals $[\omega, z]$ represent all the exogenous inputs including the uncertainty channels and performance outputs. In preview steering control, the disturbance inputs are the road curvature and the preview input. The uncertainty inputs also enter from this channel to the system when the uncertain state space models are used. The transfer function of this input-output pair $T_{\omega z}$ is minimized while satisfying the stability conditions. The state (or static output) feedback controller produce the feedback control signal (u) from the measured output (v) of the plant. The robust control norm minimization can be computed using LMI convex optimization methods by the Lyapunov stability theory. In this context, a closed loop discrete time system (11) is asymptotically stable if and only if there exists a positive symmetric matrix $\mathcal{P}$ satisfying the LMI given by Equation (12).

$$\begin{aligned} x(k+1) &= \mathcal{A}x + \mathcal{B}w \\ z(k) &= \mathcal{C}x + \mathcal{D}w \end{aligned} \quad (11) \qquad \begin{bmatrix} \mathcal{P} & \mathcal{A}\mathcal{P} \\ \mathcal{P}\mathcal{A}^\mathcal{T} & \mathcal{P} \end{bmatrix} > 0 \quad (12)$$

Similarly, the parameter dependent system models and Lyapunov matrix solution are defined for the LPV systems as;

$$\begin{aligned} x(k+1) &= \mathcal{A}(\rho)x + \mathcal{B}(\rho)w \\ z(k) &= \mathcal{C}(\rho)x + \mathcal{D}(\rho)w \end{aligned} \quad (13) \qquad \begin{bmatrix} \mathcal{P}(\rho) & \mathcal{A}(\rho)\mathcal{P}(\rho) \\ \mathcal{P}(\rho)\mathcal{A}(\rho)^\mathcal{T} & \mathcal{P}(\rho) \end{bmatrix} > 0 \quad (14)$$

where the script letters in (13) represent the closed loop system matrices (15) and ρ is the varying parameters.

$$\begin{bmatrix} \mathcal{A} := A(\rho) + B(\rho)K(\rho) & \mathcal{B} := B_w(\rho) \\ \mathcal{C} := C_z(\rho) + D_{zu}(\rho)K(\rho) & \mathcal{D} := D_{zw}(\rho) \end{bmatrix} \quad (15)$$

In polytopic system model approach, parameter variations are bounded by polytopes with a number of vertices. In this case, the model for any value of the varying parameters is obtained as a convex combination of the linear models computed at the polytope vertices ω_i [22]. The polytopic representation of a system is given as;

$$\Sigma_{LPV} = Co\left\{ \sum_{i=1}^{p} \alpha_i \begin{bmatrix} \mathcal{A}(\omega_i) & \mathcal{B}(\omega_i) \\ \mathcal{C}(\omega_i) & \mathcal{D}(\omega_i) \end{bmatrix} \right\} \quad (16)$$

where $\sum_{i=1}^{p} \alpha_i = 1$ and $\alpha_i > 0$, α_i are the barycentric coordinates in the polytope and computed by linear programming or least square methods. The controllers are computed from the closed loop solution as shown in the next subsection.

A. Robust Preview Steering Control Gain Scheduling

The vehicle longitudinal speed is measured real-time and is chosen as the scheduling parameter. The speed dependent polytopic models are then constructed by choosing a speed interval. In this application, the speed varies between 3-30 m/s. The lower limit is fixed at 3 m/s is due to the preview length. At the lower speeds the preview length becomes shorter as it is dependent on the vehicle speed. We use 50 Hz sampling frequency for discrete system and one second preview horizon. At lower speeds such for 1-2 m/s the preview distance corresponds to 1-2 meter which does not contribute much to the controller performance at lower speeds while reducing the controller performance at higher speeds. The real time controller coefficients are computed as the linear combination of all vertice point controllers.

Upper value of the speed interval can be changed at a cost of higher feedback coefficients. We have two varying variables both are the function of vehicle longitudinal speed (V_x and $1/V_x$). Since both of the varying parameters is a function of vehicle speed, a reduced polytope with three vertices can be constructed as shown in Fig. (3).

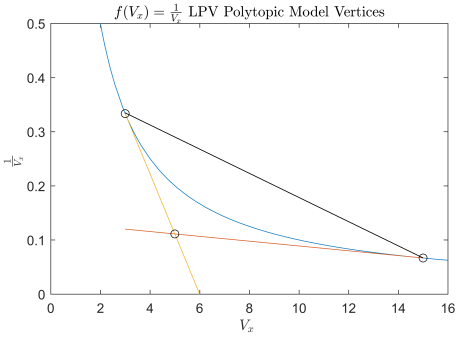

Fig. 3. Model Polytope Vertices

The first two vertex points are the boundary points of the vehicle speed. The third vertex is obtained by taking the intersection point of the lines that are tangent to the speed curve given in the figure.

In robust control, dynamic weighting filters are used to emphasize the desired frequency shapes of the sensitivity (S) and complementary sensitivity transfer T functions [23, 24]. Control weighting filters are also used to shape the desired control input frequency content. In the LQ H_∞ scheme, the weights on the state and the control signals are constant over all the frequencies. When dynamic weights are used in the optimization, both the number of filters as well as the number of parameters increase. Furthermore, the dynamic filters increase the generalized plant's dimension. The LQ synthesis is more desirable as the weighting parameters are constant at a cost of conservative solution and it is easier to tune. The generalized plant diagram of the LQ settings is given in Fig. (4).

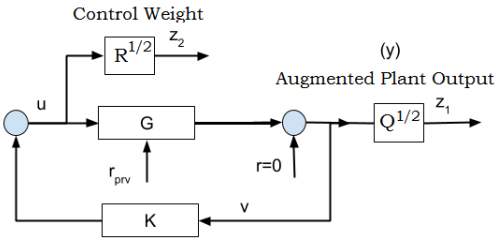

Fig. 4. Controller Synthesis - Performance Outputs with Static Weights (LQ)

The output weighting matrix $Q = diag(q_1, q_2)$ is a diagonal matrix of two parameters for the lateral deviation of the vehicle from current previewed point and heading angle errors which are defined in the measurement matrix. Two performance channels are represented by z_1 and z_2 signals in the diagram. The discrete LMI conditions for H_∞ full state feedback controllers are defined by the following matrix inequities [25, 26].

At the polytope vertices (ω_i) where $i = 1 \ldots p$, there exist symmetric positive matrices P_i and full rank matrix $Z_i \in \mathbb{R}^{1,n}$ where n is the total number of states, the following LMI conditions hold for the norm condition of a discrete transfer function from all exogenous inputs to the performance outputs $\|H_{zw}\|_2^2 < \nu$ of the system;

H_∞ ***Guaranteed Stability Conditions*** for $\|H_{zw}\|_\infty^2 < \mu$

$$\begin{bmatrix} P_i & A_i P_i + B_{u(i)} Z_i & B_{wi} & 0 \\ (\star)^T & P_i & 0 & P_i^T C_{zi}^T + Z_i^T D_{zu(i)}^T \\ (\star)^T & (\star)^T & I & D_{zw(i)}^T \\ (\star)^T & (\star)^T & (\star)^T & \mu I \end{bmatrix} > 0 \quad (17)$$

Then the controller coefficients are recovered by the barycentric coordinates using;

$$Z(\hat{\alpha}) = \textstyle\sum_i^p \alpha_i Z_i, \qquad P(\hat{\alpha}) = \textstyle\sum_i^p \alpha_i P_i, \quad K(\alpha) = Z(\hat{\alpha}) P(\hat{\alpha})^{-1} \quad (18)$$

The LMI based robust controller solutions tend to result in fast response controller in the transient region. Pole assignment or placement LMI conditions are defined in the LMI equations to shape the transient response of the system. In this study, we require the real part of the all vehicle states are greater than a positive constant. The pole region constraints for the vehicle states are derived by partitioning the Lyapunov matrices. In this case, the partitioned Lyapunov matrices are expressed as;

$$P_i = \begin{bmatrix} P_{11,i} & P_{12,i} \\ P_{12,i}^T & P_{22,i} \end{bmatrix}, P_{11,i} \in \mathbb{R}^{nv,nv}, \quad P_{22,i} \in \mathbb{R}^{nr,nr} \quad (19)$$

In Equation (19), n_v and n_r represent the number of vehicle and road preview states respectively. We can define LMI pole region for the vehicle states by the following inequalities [27]. An LMI region can be represented as a subset;

$$\mathcal{D} = \{z \in \mathbb{C} : \alpha + z\beta + \bar{z}\beta^T\}$$

where the real matrices α and β are symmetric such that $\alpha = \alpha^T$ and $\beta = \beta^T$. Similarly, $\mathcal{D}$-stable LMI regions can be defined to assign the eigenvalues of closed loop system transition matrices $A_{ve,i}$. Assume, there exist symmetric Lyapunov matrices $P_{11,i} > 0$ and the matrix valued equations for a LMI region defined by the Kronecker product operations $\otimes$;

$$\mathcal{M}_{\mathcal{D}} = \alpha \otimes P_{11,i} + \beta \otimes (P_{11,i} A_{ve,i}) + \beta^T \otimes (P_{11,i} A_{ve,i})^T$$

The positivity constraints for discrete systems can be represented by the region; $\mathcal{D}_p = \{z \in \mathbb{C} : Re(z) \geq \zeta_p \quad \zeta_p \geq 0\}$

which corresponds to the following matrix valued function $f_{\mathcal{D}_p}(z) > 0$ with

$$f_{\mathcal{D}_p}(z) = \zeta_p \begin{bmatrix} 2 & 0 \\ 0 & -2 \end{bmatrix} + \begin{bmatrix} 0 & 0 \\ 0 & 1 \end{bmatrix} z + \begin{bmatrix} 0 & 0 \\ 0 & 1 \end{bmatrix} \hat{z} \tag{20}$$

By these constraints, the eigenvalues of discrete closed loop transition matrix are assigned to have a value greater than a positive constant while the Schur stability conditions (eigenvalues of the closed loop transition matrix is less than one) are guaranteed by the LMI equations (17). The closeness of the eigenvalues to the origin of the unit disk defines the speed of transient response. The eigenvalues close the origin yield faster response.

IV. Results and Discussions

We computed preview steering state feedback controllers for a mid-range passenger car. The single track nominal parameters are known. Two sets of controllers were computed by constructing certain and uncertain vehicle models. The vehicle longitudinal speed is taken as the time varying parameter. The state feedback controllers are obtained for different speed intervals such as for the speed intervals [3-15 m/s] and [3-30 m/s]. In the uncertain vehicle models, the tire cornering coefficients are treated as the uncertain parameters. The state space uncertainty is used in the models [23]. This is easy to do in Matlab by lftdata command. The state feedback coefficients are computed with the certain and uncertain representations in LQ H_∞ solution. However for comparison, we give some results for the models where uncertainty is discarded and all the parameters are treated to be known by solving the robust optimal control problem with extended discrete LMIs given in [26].

We obtained tight tracking performance using H_∞ and H_2 norms separately with dynamic filters. Despite the satisfactory tight tracking performance, the resulting control coefficients are very high to implement and the transient response is very fast. It is the same for LQ H_∞ robust controllers. The steady state tracking error for all solutions stays in the $\pm$ 3 cm for all the speed range.

In order to slow down the transient response, it is essential to use additional eigenvalue (pole) constraints in the solution. We set a positivity constraint to push the four eigenvalues of the vehicle plant transition matrix away from origin by partitioning the Lyapunov matrix. In this way, we can obtain slower response with lower constant optimization weights by setting $Q = diag(0.95,\ 3e{-}3)$ and the control signal weight $R = 0.25$. The tracking performance and control gain results of the LQ robust control solution for nominal plant without uncertainty are given in the following figures (5) for the speed interval [3-30 m/s]. On the cornering points, the response gets smoother in Fig. 5.

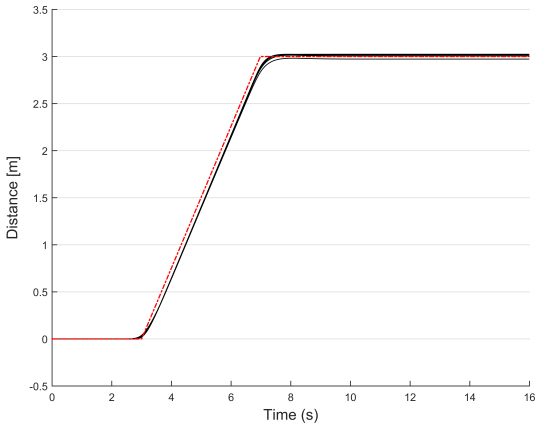

Fig. 5. H_∞ LQ Solution Tracking Performance with Constant Weights

The corresponding gain vectors (K1, K2, and K3) at each of the polytope vertices are shown in Fig. 6. The maximum level of the gains are four times lower than the case when the pole constraint is not added to the LMIs.

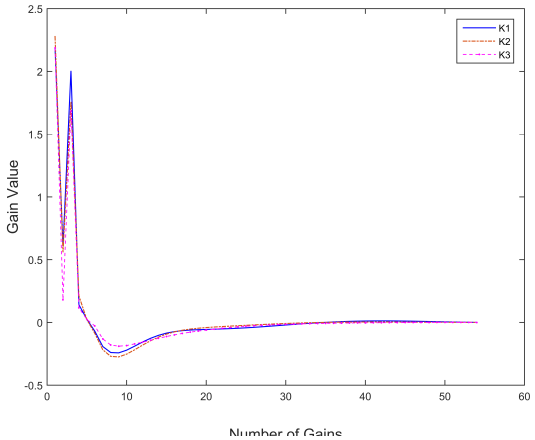

Fig. 6. H_∞ LQ solution Controller Gains

V. Conclusion

In this study we presented robust preview controllers in LQ H_∞ form for certain and uncertain plants. The robust optimization problems were then solved using constant weighting matrices. The tire cornering stiffnesses are treated as the uncertain with a range of $\pm$30 %. The resulting control and tracking performance were compared to the solutions obtained when dynamic weights were used with extended LMI formulations. The robust optimization solved in LMI

framework yielded fast transient response with high controller gains. We added eigenvalue constraints in the solution to prevent the higher gains and fast response and obtained more implementable controller with lower gains for 50 preview points. The results show that 50 preview points are sufficient in the current settings. The computational time is short when static weights are used, however, the computations get longer when the dynamic weights are used in the extended LMI framework. We conclude that, LQ H_∞ method is sufficient to obtain satisfactory results with pole constraint LMI solution.

REFERENCES

[1] D. Cole, A. Pick, and A. Odhams, "Predictive and linear quadratic methods for potential application to modelling driver steering control," *Vehicle System Dynamics*, vol. 44, no. 3, pp. 259–284, 2006.

[2] B. D. Anderson and J. B. Moore, *Linear optimal control*. Prentice-Hall Englewood Cliffs, 1971, vol. 197, no. 1.

[3] R. R. Bitmead, M. Gevers, and V. Wertz, *Adaptive optimal control: The thinking man's GPC*. Elsevier, 1990.

[4] A. Lee, "A preview steering autopilot control algorithm for four-wheel steering passenger vehicles," *TRANSACTIONS-AMERICAN SOCIETY OF MECHANICAL ENGINEERS JOURNAL OF DYNAMIC SYSTEMS MEASUREMENT AND CONTROL*, vol. 114, pp. 401–401, 1992.

[5] R. S. Sharp, "Optimal linear time-invariant preview steering control for motorcycles," *Vehicle system dynamics*, vol. 44, no. sup1, pp. 329–340, 2006.

[6] K. Takaba, "Robust servomechanism with preview action for polytopic uncertain systems," *International Journal of Robust and Nonlinear Control*, vol. 10, no. 2, pp. 101–111, 2000.

[7] M. Tomizuka, ""optimum linear preview control with application to vehicle suspension"—revisited," *Journal of Dynamic Systems, Measurement, and Control*, vol. 98, no. 3, pp. 309–315, 1976.

[8] N. Louam, D. Wilson, and R. Sharp, "Optimal control of a vehicle suspension incorporating the time delay between front and rear wheel inputs," *Vehicle system dynamics*, vol. 17, no. 6, pp. 317–336, 1988.

[9] G. Prokop and R. Sharp, "Performance enhancement of limited-bandwidth active automotive suspensions by road preview," *IEEE Proceedings-Control Theory and Applications*, vol. 142, no. 2, pp. 140–148, 1995.

[10] R. Sharp and V. Valtetsiotis, "Optimal preview car steering control," *Vehicle System Dynamics*, vol. 35, pp. 101–117, 2001.

[11] R. Rajamani, *Vehicle dynamics and control*. Springer Science & Business Media, 2011.

[12] A. Hazell, "Discrete-time optimal preview control," Ph.D. dissertation, University of London, 2008.

[13] K. Takaba, "A tutorial on preview control systems," in *SICE 2003 Annual Conference*, vol. 2. IEEE, 2003, pp. 1388–1393.

[14] L. Saleh, P. Chevrel, and J.-F. Lafay, "Optimal control with preview for lateral steering of a passenger car: Design and test on a driving simulator," in *Time Delay Systems: Methods, Applications and New Trends*. Springer, 2012, pp. 173–185.

[15] L. Mianzo and H. Peng, "Output feedback preview control of an electromechanical valve actuator," *IEEE Transactions on Control Systems Technology*, vol. 15, no. 3, pp. 428–437, 2007.

[16] A. Moran Cardenas, J. G. Rázuri, I. Bonet, R. Rahmani, and D. Sundgren, "Design of high accuracy tracking systems with h_∞ preview control," *Polibits*, no. 50, pp. 21–28, 2014.

[17] M. Thommyppillai, S. Evangelou, and R. Sharp, "Car driving at the limit by adaptive linear optimal preview control," *Vehicle system dynamics*, vol. 47, no. 12, pp. 1535–1550, 2009.

[18] H. Peng and M. Tomizuka, "Preview control for vehicle lateral guidance in highway automation," *Journal of Dynamic Systems, Measurement, and Control*, vol. 115, no. 4, pp. 679–686, 1993.

[19] N. Paulino, C. Silvestre, and R. Cunha, "Affine parameter-dependent preview control for rotorcraft terrain following flight," *Journal of guidance, control, and dynamics*, vol. 29, no. 6, pp. 1350–1359, 2006.

[20] M. ApS, *The MOSEK optimization toolbox for MATLAB manual. Version 7.1 (Revision 28).*, 2015. [Online]. Available: \url{http://docs.mosek.com/7.1/toolbox/index.html}

[21] J. Lofberg, "Yalmip: A toolbox for modeling and optimization in matlab," in *Computer Aided Control Systems Design, 2004 IEEE International Symposium on*. IEEE, 2004, pp. 284–289.

[22] O. Sename, P. Gaspar, and J. Bokor, *Robust control and linear parameter varying approaches: application to vehicle dynamics*. Springer, 2013, vol. 437.

[23] K. Zhou, J. C. Doyle, K. Glover *et al.*, *Robust and optimal control*. Prentice hall New Jersey, 1996, vol. 40.

[24] S. Skogestad and I. Postlethwaite, *Multivariable feedback control: analysis and design*. Wiley New York, 2007, vol. 2.

[25] K. Zhou, P. P. Khargonekar, J. Stoustrup, and H. H. Niemann, "Robust performance of systems with structured uncertainties in state space," *Automatica*, vol. 31, no. 2, pp. 249–255, 1995.

[26] M. C. De Oliveira, J. C. Geromel, and J. Bernussou, "Extended h_2 and h_∞ characterizations and controller parametrizations for discrete-time systems," *International Journal of Control*, vol. 75, no. 9, pp. 666–679, 2002.

[27] M. Chilali, P. Gahinet, and P. Apkarian, "Robust pole placement in lmi regions," *IEEE Transactions on Automatic Control*, vol. 44, no. 12, pp. 2257–2270, 1999.